Ecotoxicology and Environmental Safety 223 (2021) 112584

Contents lists available at ScienceDirect

Ecotoxicology and Environmental Safety

journal homepage: www.elsevier.com/locate/ecoenv

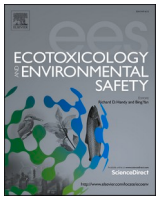

Impact of selenium on cerebellar injury and mRNA expression in offspring of rat exposed to methylmercury

Rui Tu [a,b,c], Chanchan Zhang [b], Ling Feng [b], Huiqun Wang [b], Wenjuan Wang [b,*], Ping Li [a,*]

[a] State Key Laboratory of Environmental Geochemistry, Institute of Geochemistry, Chinese Academy of Sciences, Guiyang 550081, China
[b] Key Laboratory of Environmental Pollution Monitoring and Disease Control/School of Public Health, Guizhou Medical University, Guiyang 550025, China
[c] Division of Infection Management, Guiyang First People's Hospital, Guiyang 550000, China

ARTICLE INFO

Edited by Professor Bing Yan

Keywords:
Methylmercury
Selenium
Rat
Histopathology
MRNA

ABSTRACT

During the fetal development stage, the Central Nervous System (CNS) is particularly sensitive to methylmercury (MeHg). However, the mechanism underlying the antagonistic effect of selenium (Se) on MeHg toxicity is still not fully understood. In this study, female rat models with MeHg and Se co-exposure were developed. Pathological changes in the cerebellum and differential mRNA expression profiles in offspring rats were studied. In the MeHg-exposed group, a large number of Purkinje cells showed pathological changes and mitochondria were significantly swollen; co-exposure with Se significantly improved the structure and organization of the cerebellum. In total, 378 differentially expressed genes (DEGs) (including 284 up-regulated genes and 94 down-regulated genes) in the cerebellum of the MeHg-exposed group and 210 DEGs (including 84 up-regulated genes and 126 down-regulated genes) in the cerebellum of the MeHg+Se co-exposed group were identified. The genes involved in neurotransmitter synthesis and release and calcium ion balance in the cerebellum were significantly up-regulated in the MeHg-exposed group. These genes in the MeHg+Se co-exposed group were not changed or down-regulated. These findings demonstrate that the neurotoxicity caused by MeHg exposure is related to the up-regulation of multiple genes in the nerve signal transduction and calcium ion signal pathways, which are closely related to impairments in cell apoptosis and learning and memory. Supplementation with Se can mitigate the changes to related genes and protect neurons in the mammalian brain (especially the developing cerebellum) from MeHg toxicity. Se provides a potential intervention strategy for MeHg toxicity.

1. Introduction

Mercury (Hg) is one of the most hazardous chemical elements in the environment. Hg pollution comes from a wide range of sources, and the process of Hg migration and transformation in the environment is complex. Hg pollution lasts for a long time and it is difficult to eliminate (Mergler et al., 2007). Methylmercury (MeHg) is lipophilic, which can be circulated and enriched through the biological chain, and exhibited increased toxicity. Since humans are the terminal of the food chain, MeHg eventually enters the human body and poses a threat to human health (Wells et al., 2016). Minamata disease in Japan in the 1950s was caused by MeHg exposure, and increased attention has been directed towards MeHg toxicity (Driscoll et al., 2013).

MeHg has a high affinity to thiol-containing enzymes and proteins, and can damage the nervous system (Pamphlett et al., 2019), immune system (Osuna et al., 2014), cardiovascular system (Genchi et al., 2017), kidneys (Sun et al., 2019) and even DNA (Grotto et al., 2009)through the blood-brain barrier and placental barrier. MeHg accumulates mainly in the central nervous system (CNS), with the cerebellum being one of the most severely affected areas. Previous studies have observed that the effects of MeHg on neurotransmitter systems (Kaur et al., 2007), Ca^{2+} ion homeostasis (Johansson et al., 2007), and free radical-induced oxidative damage produced by C-Hg bond cleavage are the main mechanisms underlying MeHg neurotoxicity (Franco et al., 2007). In particular, the developing fetal brain, which has an underdeveloped blood-brain barrier and exhibits rapid growth, proliferation, and differentiation (Sakamoto et al., 2018), is more sensitive to MeHg than the adult brain.

Early studies have found that the presence of Se can protect marine mammals from the toxic damage of MeHg (Koeman et al., 1973). Since then, Se has received the most attention as a potential protective agent against MeHg toxicity. The physicochemical properties of Se are similar

* Corresponding authors.
E-mail addresses: reality0337@126.com (W. Wang), liping@mail.gyig.ac.cn (P. Li).

https://doi.org/10.1016/j.ecoenv.2021.112584
Received 5 April 2021; Received in revised form 20 July 2021; Accepted 29 July 2021
Available online 5 August 2021

to those of sulfur, because Se can replace the sulfur atom in sulfide to form a stronger Hg-Se complex with Hg, which inhibits the oxidation process in the body and reduces the toxicity of MeHg (Karita et al., 2016; Ralston and Raymond, 2010). Supplementation with organic Se can alleviate lipid peroxidation and DNA damage caused by Hg exposure in humans (Li et al., 2012). Further, selenium methionine (SeMet) protects against neuronal degeneration caused by MeHg exposure in seven-day-old Sprague Dawley (SD) rats (Sakamoto et al., 2013).

There is a large body of published literature on the mutual attenuation of Hg and Se toxicity in experimental animals. However, these studies have focused on changes to the forms of Hg and Se in organisms; moreover, Hg-Se complexes have only been demonstrated experimentally. Few studies have reported on the molecular mechanisms underlying Hg-Se interactions. It is not clear whether the interaction between Hg and Se in the body is a multi-cell or multi-gene complex network mediation pathway. This study was designed to evaluate the protective effects of SeMet supplement on the offspring of female rats exposed to MeHg. High-throughput sequencing technology was used to study the mRNA expression profiles in the cerebellum of the pups, and the differences in gene function and signaling pathways were analyzed. The results of this study can provide new insight into the potential value of Se in MeHg-induced neurotoxicity and the possible mechanism.

2. Materials and method

2.1. Animal models

The number of rats used in this experiment was designed according to the 3Rs principle proposed by Tain et al. (2017). SD rats (12 females and 12 males) aged four weeks were obtained from the Experimental Animal Center, Guizhou Medical University, China. Ethical approval for this study was granted by the Bioethical Committee of the Institute of Animal Care Committee, Guizhou Medical University, China (Permit No. SYXKA(Q)2012–0001), and the study was performed in accordance with the National Institute's guidelines for animal care and use. All efforts were made to minimize the number of animals used and their suffering. Rats were maintained under a 12 h light/dark cycle and were housed for seven days prior to receiving experimental treatment. Male rats were removed on day 1 of gestation (GD) and 12 females were randomly divided into four groups (n = 3 per group): Control (0.9% NaCl solution), Se-exposed (0.2 mg Se/kg/day), MeHg-exposed (1.2 mg MeHg/kg/day), and MeHg+Se co-exposed (1.2 mg MeHg/kg/day + 0.2 mg Se/kg/day), and corresponding chemicals were taken by gavage. The dosage level of MeHg was adopted from the literature, since the oral LD_{50} of rat was 58 mg/kg methyl chloride (Chang, 1996). A 1/50 LD_{50} (1.2 mg MeHg/kg/day) adopted for this experiment, which is a neurotoxic dose of MeHg used for model rats (Beyrouty and Chan, 2006; Sakamoto et al., 2013). The maximum tolerated dose (MTD) of SeMet in adult rats is 2 mg Se/kg/day (Tsunoda et al., 2000), and the relatively safe dose of 1/10 MTD (0.2 mg Se/kg/day) was selected as the experimental dose. Parent female rats were continuously exposed to the corresponding doses of MeHg and Se for 8 weeks before mating, during pregnancy and lactation, until the end of weaning exposure at 21 days after birth. During this period, each group rats were housed individually in a cage to monitor mother's daily diet and water intake.

2.2. Sample collection

On postnatal day 21 (PND21), offspring rats were anesthetized with 2% sodium pentobarbital, and brain tissues were quickly removed and placed on ice to isolate the cerebellum. The cerebellum tissues of offspring rats were taken from different litters from each group and placed in RNA protection solution. Specimens were then placed in a refrigerator at 4 ℃ overnight. After this, the tissues were completely infiltrated with RNA protection solution. The tissues were then stored at − 80 ℃ before total RNA extraction. The cerebellum tissue was fixed in 10% neutral formalin solution for HE staining. In each group, the cerebellum tissue was fixed in 2.5% glutaraldehyde, and stored at 4 ℃ for the experiments of transmission electron microscope. The remained cerebellar tissues ware stored in a refrigerator at − 80 ℃ for further use.

2.3. Hg and Se analysis

The cerebellum samples were digested using HNO_3 at 95 ℃ for 3 h, and the total Hg (THg) concentrations in the digested solutions were measured using BrCl oxidation, $SnCl_2$ reduction, and cold vapor atomic fluorescence spectrometry (CVAFS) detection. The cerebellum tissues were digested in HNO_3 at 150 °C for 16 h, dried at 110 °C on a hot plate, and reduced with 3 mL HCl (6 mol/L). The Se concentrations were determined by hydride generation atomic fluorescence spectrometry (AFS-230E, Haiguang, China)(Zhu et al., 2008).

2.4. Morphological analysis

The cerebellum samples were fixed in 10% formaldehyde for 48 h, dehydrated by graded ethanol, and embedded in paraffin. Then, the samples were cut into 4 μm sections and stained with hematoxylin and eosin (H&E). Sections were observed under an optical microscope for histopathological determination.

The cerebellums of offspring were removed completely and cut into small pieces of 1 mm^3. The tissues were immersed in 2.5% glutaraldehyde fixing solution (containing 0.1 M phosphoric acid buffer solution and 4% paraformaldehyde) for 2 h at 4 ℃. They were then washed with 0.1 M phosphoric acid buffer solution, dehydrated by ethanol gradient, replaced ethanol with oxypropane, and then soaked and embedded in epoxy resin Epon812. The ultrathin sections (50–70 nm) were stained and further observed and photographed under a JEM-100SX transmission electron microscope.

2.5. Sequencing data analysis

2.5.1. Analysis of differentially expressed Gene (DEGs)

The DEGs of the four groups (four biological replicates per group) were analyzed by edgeR (Robinson and Oshlack, 2010) and the P-values were obtained. After multiple hypothesis tests were performed, the threshold P-value was determined by controlling the false discovery rate (FDR). At the same time, multiple differential expressions were calculated according to the FPKM (Fragments Per Kilobase of exon model per Million mapped reads) value, that is, the fold-change. In order to explore the DEGs, the expression level of each gene was calculated by introducing FPKM values, and the differential gene screening conditions were defined: 1) fold-change$\geq$ 2 and *P*-value$\leq$ 0.05 was defined as significantly up-regulation; 2) fold-change$\leq$ −2 and *P*-value$\leq$ 0.05 was defined as significant down-regulation.

2.5.2. Enrichment analysis of Kyoto Encyclopedia of Genes and Genomes (KEGG)

The Genecluster 2.0 and Cluster 3.0 packages were used to perform enrichment analysis of DEGs. The principle of KEGG enrichment analysis is to map the selected DEGs to each term in the KEGG database, calculate the gene number of each term, and then apply hypergeometric tests. Relative to the whole genome background, KEGG terms that were significantly enriched in DEGs were screened.

To evaluate the possible regulation mechanisms of dysregulated mRNAs, as well as their relationships in the process of MeHg toxicity, KEGG pathway analysis was performed. KEGG pathway analysis reflects the location and expression trends of differential genes in known signaling pathways, which reveals the interaction between differential genes. Based on the KEGG database, the DEGs in each group were analyzed by chi-square test. The signal pathways involved in the target differential genes were analyzed. *P*-value$<$ 0.05 was used to determine the significance of the participation of differential genes in each group.

2.6. Statistical analysis

The data are described as mean ± standard deviation (SD) and were analyzed using SPSS 20.0 for Windows. One-way analysis of variance (ANOVA) was used to examine differences between different groups. The results of the statistical tests were considered to be statistically significant when $p < 0.05$.

3. Results and discussion

3.1. Animal model

Temporal changes in the body weights of parental female rats are shown in Table S1. The MeHg-exposed group had a significantly ($p < 0.05$) lower average body weights than the control group during the pre-mating, gestation, and lactation periods. In the MeHg-exposed group, the parental female rats showed a decrease in dietary intake and delayed pregnancy. No significant differences in the growth index and eating habits of the parental female rats were observed between the MeHg+Se co-exposed group, Se-exposed group, and the control group. Increases in body weights in the MeHg-exposed group were much slower than those in the control group and the MeHg+Se co-exposed group.

The average number of litters size of parental female rats in the control group, Se-exposed group, MeHg-exposed group, and MeHg+Se co-exposed group were 14.7 ± 0.6, 13.3 ± 1.5, 10.7 ± 0.6 and 12.3 ± 0.6, respectively. The survival rates of offspring rats during lactation are shown in Fig. S1. From postnatal day (PND) 1–7 and from PND7 to PND21, the average survival rates of offspring rats in the MeHg exposed group were 53.4% and 77.6%, respectively. No postnatal deaths were observed in the control group, Se-exposed group, and MeHg+Se co-exposed group.

Temporal changes in body weight in the offspring rats are shown in Table 1. The MeHg-exposed group had significantly ($p < 0.05$) lower average body weights than the control group at PND3, PND7, and PND14. However, the MeHg+Se co-exposed group had significantly ($p < 0.05$) higher average body weights than the MeHg-exposed group at PND7 and PND14.

Se supplementation significantly increased the growth and survival rate of the pups in the MeHg+Se co-exposed group compared with the MeHg-exposed group. The results showed that supplemental Se could mitigate the growth impairment resulting from MeHg toxicity. This is consistent with the previous studies, which showed that the MeHg-induced mortality and reduced fetal weight were mitigated by Se supplementation (Sakamoto et al., 2013).

3.2. Hg and Se concentration

THg concentrations in the brains of the control group, Se-exposed group, MeHg-exposed group, and MeHg+Se co-exposed group averaged at 0.006 ± 0.004 μg/g, 0.004 ± 0.003 μg/g, 0.822 ± 0.157 μg/g, and 1.40 ± 0.223 μg/g, respectively. The offspring of MeHg-exposed group, and MeHg+Se co-exposed group were not directly exposed to MeHg, but indirectly exposed to MeHg through the placenta and breast milk of the parental female rats. The THg and Se concentrations in the brains of offspring rat are shown in Fig. 1. The brain THg concentrations in offspring of the MeHg-exposed group were significantly higher than those of the control group ($p < 0.05$). The average of THg concentrations in the brains of the MeHg+Se co-exposed group was significantly higher (1.7 times) than that of the MeHg-exposed group ($p < 0.05$). No significant difference of THg concentrations in the brains was found between the control group and the Se-exposed group ($p > 0.05$).

The Se concentrations in the brains of the control group, Se-exposed group, MeHg-exposed group and MeHg+Se co-exposed group were 0.150 ± 0.018 μg/g, 0.368 ± 0.020 μg/g, 0.1876 ± 0.005 μg/g, and 0.844 ± 0.109 μg/g, respectively. The Se concentrations in the brains of the Se-exposed group were significantly ($p < 0.05$) higher than those of the control group. The average of Se concentrations in the brains of the MeHg+Se co-exposed group was significantly higher (2.3 times) than that of the Se exposed group ($p < 0.05$).

The average of THg concentration in the MeHg+Se co-exposed group was 1.7 times that of the MeHg-exposed group, and the average Se concentration in the MeHg+Se co-exposed group was 2.3 times that of the Se-exposed group. Combined exposure to MeHg and Se significantly increased the accumulation of Hg and Se in the cerebellum of offspring rats. These results are consistent with a previous study which investigated the effect of Se on MeHg-induced brain degenerative changes in seven-day-old rats. The Hg and Se levels in the brain tissue of the MeHg and Se co-exposed group were higher than those of the MeHg (or Se)-exposed group alone (Sakamoto et al., 2013). The physical and chemical properties of Se are similar with those of sulfur. The Se in food intake may be directly metabolized into active Se or selenomethionine to replace the sulfur-containing methionine in tissue protein; then, the reactive Se forms a complex with MeHg in the liver (Schrauzer, 2000). The reaction between MeHg and the Se amino acid to form dimethylmercury selenide may be the mechanism underlying MeHg demethylation (Karita et al., 2016). Ralston et al. found that the MeHg and Se complex form may be MeHg-selenocysteine, which is similar to MeHg-cysteine and can easily enter the brain tissue (Ralston and Raymond, 2010). The specific complex formed by the combination of MeHg and Se requires clarification in future studies. Although the co-exposure to MeHg and Se increased the accumulation of Hg and Se in the rat body, the complex formed by MeHg and Se protected neurons from the damage induced by MeHg.

Table 1
Temporal changes in body weight in the offspring rats.

Group	PND 3 (g)	PND 7 (g)	PND 14 (g)	PND 21 (g)
Control	7.5 ± 0.8	10.9 ± 1.2	24.2 ± 2.1	35.3 ± 3.9
Se	7.0 ± 0.4	10.5 ± 1.3	22.7 ± 1.8	34.0 ± 4.7
MeHg	6.7 ± 0.4*	9.4 ± 0.8*	20.6 ± 2.7*	32.2 ± 4.7
MeHg+Se	7.1 ± 0.5	10.9 ± 0.6#	24.0 ± 2.2#	33.4 ± 4.2

PND: postnatal day. Data are expressed as the mean ± standard deviation.
* $p < 0.05$, compared with the control group.
# $p < 0.05$, compared with the MeHg exposed group.

3.3. Histomorphology

The light micrographs of the cerebellum sections are shown in Fig. 2. No obvious neuronal damage was found in the cerebellums of the control group (Fig. 2A), Se-exposed group (Fig. 2B), and MeHg+Se co-exposed group (Fig. 2D). However, in the MeHg-exposed group, more Purkinje cells were irregularly arranged and enclosed by a wide vesicular zone where necrotic cells penetrated the granular layer. The pericellular spaces were significantly widened. The cytoplasm staining deepened, and the cell structures were blurred. The nucleuses were condensed and deep and even blurred or absent in some cases (Fig. 2C).

The results of ultrastructure of the cerebellum are shown in Fig. 3. No significant alteration in the cerebellum was observed in the control group and Se-exposed group (Fig. 3A and B). In the MeHg-exposed group, endoplasmic reticulum with fragmentation or vesicular roughness in the cytoplasm were observed and the chromatin in the nucleus was slightly agglutinated; multiple swollen mitochondria were also seen in the cytoplasm (Fig. 3C). However, in the MeHg+Se co-exposed group, the structures and organizations of the cerebellum were significantly improved (Fig. 3D).

In this study, there is no significant difference in size, shape and color of the brain tissue of the offspring exposed to MeHg compared with the control group by visual observation. HE staining of cerebellar slices, observation under a 400 × optical microscope showed that Purkinje cells in the MeHg exposure group had obvious pathological changes and signs of death. This may be due to the increased accumulation of

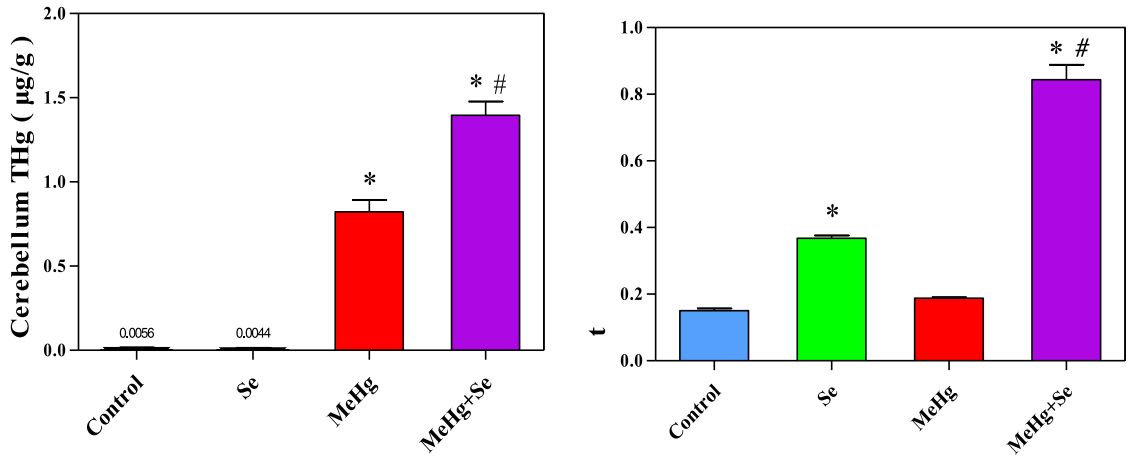

Fig. 1. THg and Se concentrations in the rat offspring brain of different groups. *$p < 0.05$, Compared with the control group; # $p < 0.05$, Compared with the MeHg group.

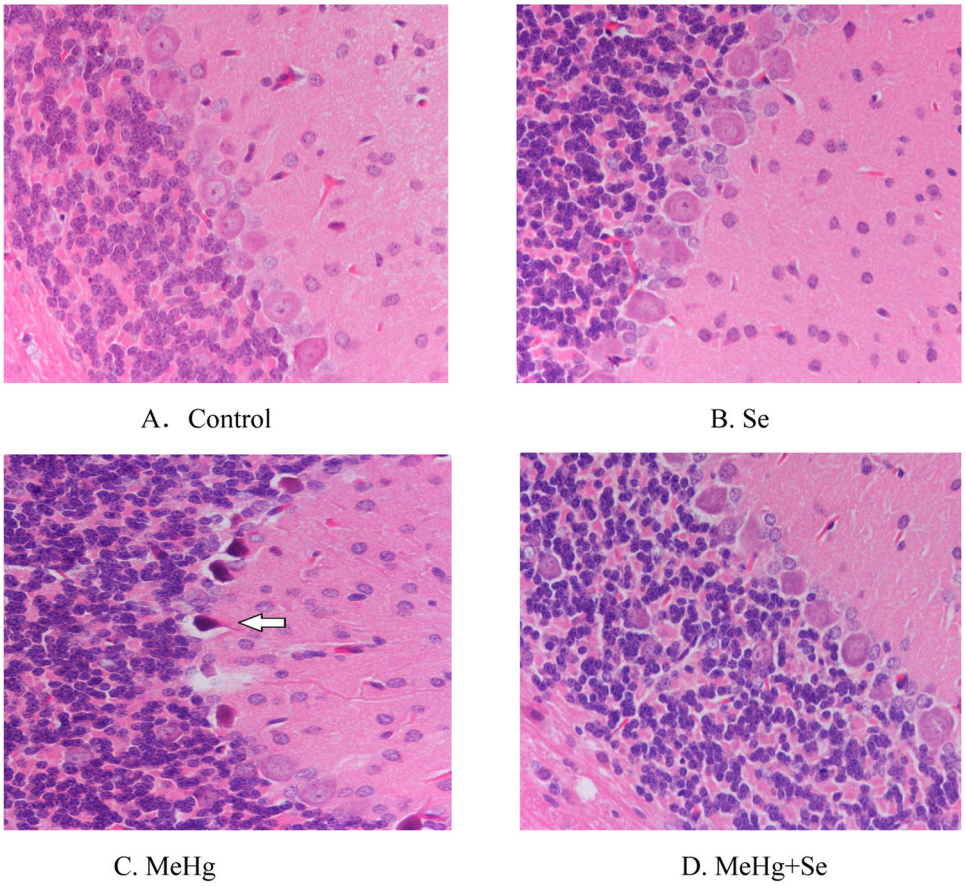

Fig. 2. Light micrographs of HE staining of the cerebellum of different groups (×400).

unfolded proteins leading to the development of oxidative stress and calcium overload. This is reflected by impairments to cognition and cerebellar function assessed by alterations in cerebellar 5-hydroxytryptamine (5-HT), dopamine (DA), and gamma-aminobutyric acid (GABA) signaling pathways. In addition, the observed mitochondrial disruption may trigger the production of cytoplasmic and mitochondrial free radicals, thereby disrupting nuclear chromatin.

MeHg has significant impacts on the structure and function of mitochondria, which reported decrease mitochondrial ATPase activity and change mitochondrial ultrastructural variables with increasing of MeHg dose (Dantzig, 2003) Under its lipophilic action, MeHg can penetrate the synaptosome membrane and damage the mitochondrial inner membrane, leading to the uncoupling of oxidative phosphorylation, reduction in ATP production, and inhibition of the synthesis of synaptosome proteins (Dreiem and Seegal, 2007). The results obtained by transmission electron microscopy revealed that Se supplementations obviously benefit the swelling of membranous organelles which caused by MeHg exposure, because Se and MeHg can form a complex to reduce the toxicity of MeHg. Further, Se can up-regulate the activity of signal transducer and activator of transcription 3 (STAT3) in cells. STAT3

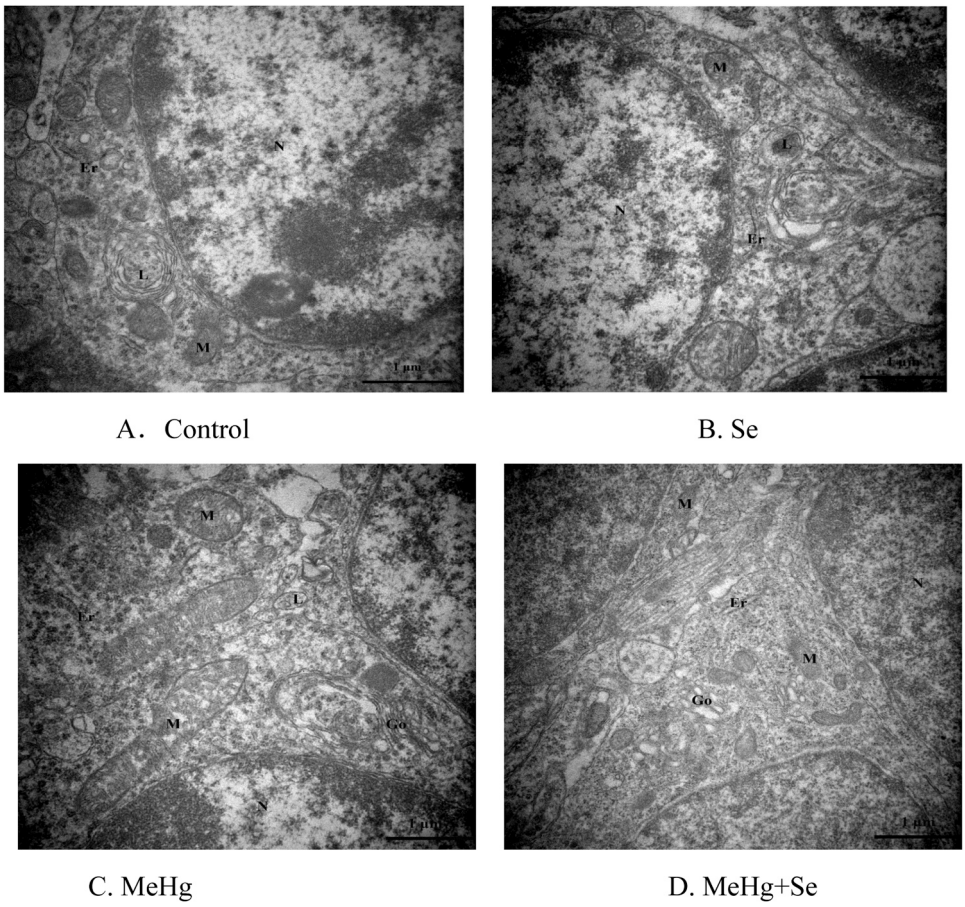

Fig. 3. Transmission electron microscope of the cerebellum of different groups. M, mitochondria; L, lysosome/ peroxisome; Go, golgi apparatus; N, nucleus; Er, endoplasmic reticulum.

works together with mitochondrial respiratory chain complex I, which plays a very important role in maintaining the electron transport chain complex and stabilizing intracellular ATP levels to maintain the protective function of normal mitochondria (Lee et al., 2014). In summary, these findings suggest that Se protect against MeHg-induced damage both at the cellular and ultrastructural level.

3.4. mRNA Expression

DEGs in different sets of sequencing samples are shown as volcanic

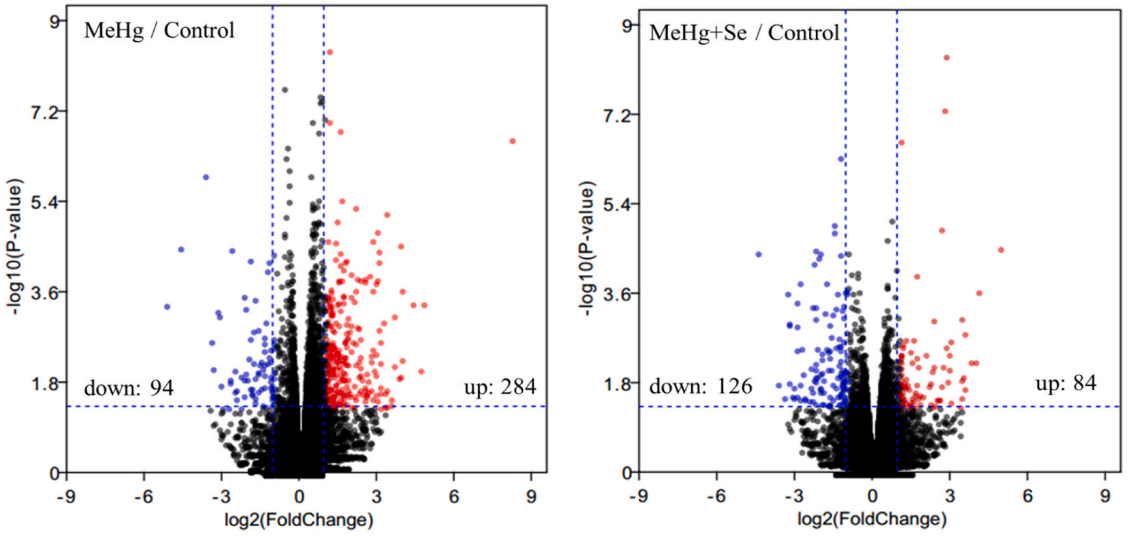

Fig. 4. Volcano plots of the total gene expression profiles of cerebellum of offspring. Significantly upregulated and downregulated genes are shown as a red and blue dot, respectively. The black dot represents no significant difference between the expressions of genes. (For interpretation of the references to color in this figure legend, the reader is referred to the web version of this article.)

distributions in Fig. 4. Compared with the control group, 378 DEGs were observed in the MeHg exposed-group, including 284 up-regulated genes and 94 down-regulated genes. Compared with the control group, 210 DEGs were observed in the MeHg+Se co-exposed group, including 84 up-regulated genes and 126 down-regulated genes. The number of differential genes in the MeHg+Se co-exposed group was much lower than that in the MeHg-exposed group. These results indicate that Se supplementation may have a restorative effect on the changes in the mRNA profile in the cerebellum caused by MeHg exposure.

Differential genes in each group were subjected to pathway analysis. The top 30 pathways were ranked according to the P-value and enrichment score, and then KEGG enrichment analysis of the DEGs was performed to interpret the biological functions and molecular pathways of the DEGs (Fig. 5A and B). Among the 73 pathways in the MeHg-exposed group, the top 10 were mainly the up-regulated DEGs: neuroactive ligand-receptor interaction (Fig. S2), calcium signaling pathway (Fig. S3), serotonergic synapse, morphine addiction, and tryptophan metabolism, mature - onset diabetes of the young, gastric acid secretion, nicotine addiction, taste transduction, and histidine metabolism neuroactive (Table S2). Among the 58 pathways in the MeHg+Se co-exposed group, the top 10 molecular pathways were mainly down-regulated DEGs: autoimmune thyroid disease, antigen processing and presentation, allograft rejection, viral myocarditis, graft-versus-host disease, herpes simplex infection, phagosome, cell adhesion molecules (CAMs), type I diabetes mellitus, and influenza A (Table S3).

Among the 34 genes associated with "neuroactive ligand-receptor interaction" by GO analysis, we focused on the genes related to neuronal information transmission. The signaling pathway of "neuroactive ligand-receptor interaction" contains a total of 211 genes, and the involved receptors can be divided into four categories: class A (rhodopsin-like), class B (secretin-like), class C (pro-metabolic glutamate/pheromone), and ion channels/other receptors. Class A biogenic amines (Michalski et al., 2021) are important stimulating nerve tissue molecules that bind to the corresponding receptors and control and regulate many important biological functions such as circadian rhythm, endocrine, cardiovascular control, mood, learning, and memory. In this study, 34 DEGs in the neuroactive ligand-receptor interaction pathway were found in the MeHg-exposed group, in which the expression of multiple receptor genes in the class A biogenic amines were up-regulated: Htr1a, Chrm2, Chrm4, Chrm5, Drd2, and Drd4.

Htr1a (5-hydroxytryptamine receptor 1a, a serotonin 1a receptor) is a subtype of serotonin receptor that binds to the neurotransmitter serotonin, it can cause G-protein coupled receptors to couple with Gi proteins and mediate inhibitory neurotransmitters, mainly with nerves regulation, endocrine, and autoreceptive effects (Liu et al., 2019). 5-HT1A receptors are present in many areas of the brain, including

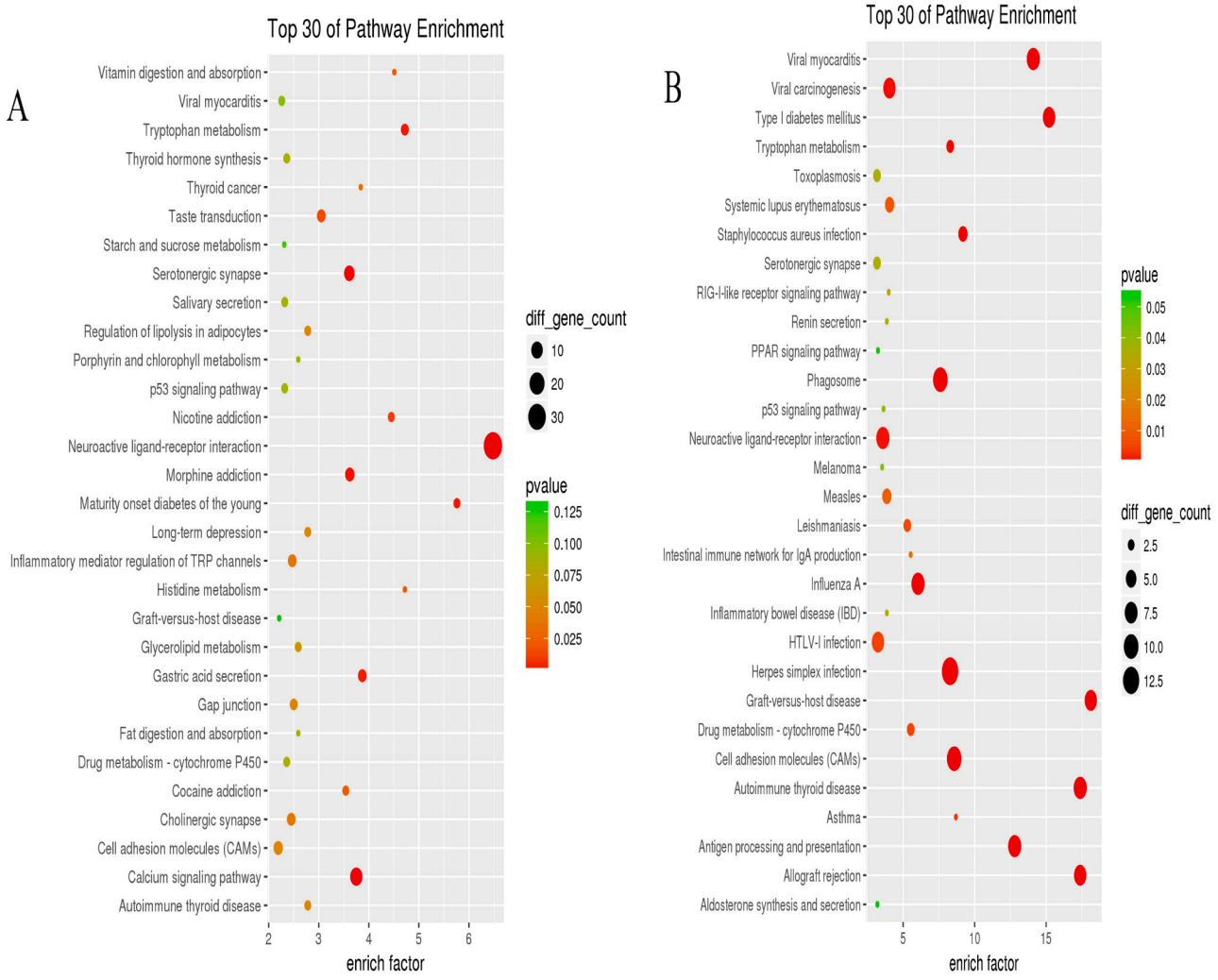

Fig. 5. Top 30 KEGG pathway analysis of differentially expressed genes in the MeHg exposed (A) and MeHg+Se co-exposed (B) groups. The vertical axis indicates the name of the KEGG pathway, and the horizontal axis indicates the enrichment factor of the KEGG pathway in the transcriptome; the circle size indicates the total number of genes present in the transcriptome, and the color shade indicates the size of the *P*-value. (For interpretation of the references to color in this figure legend, the reader is referred to the web version of this article.)

presynaptic and postsynaptic localization in the cerebral cortex. At the presynaptic level, activation of 5-HT1a receptors inhibits glutamate release, which may contribute to many neurologic and neuropsychiatric disorders (Buhot et al., 2000; Joseph and Thomsen, 2017; Yeh et al., 2020).

Chrm (cholinergic receptor muscarinic) is a gene encoding the muscarinic acetylcholine receptor (M receptor), and includes five subtypes of M1, M2, M3, M4, and M5. The corresponding coding genes are Chrm1, Chrm2, Chrm3, Chrm4, and Chrm5 (Kruse et al., 2012). Acetylcholine is the most important class of neurotransmitter in the CNS, which can activate the cerebral cortex and promote learning. M1 and M4 are postsynaptic receptors which increase the release of acetylcholine and positively regulate learning and memory. M2 is a presynaptic receptor which negatively regulates the release of acetylcholine and impact learning and memory (Joseph and Thomsen, 2017). Drd2 (dopamine receptor D2) and Drd4 (dopamine receptor D4) are members of the G-protein coupled receptor superfamily. Drd2 and Drd4 are associated with cognitive performance and cognitive deficits following traumatic brain injury. In general, Drd2 activation is associated with increased cognitive performance, while Drd4 is associated with decreased performance (Lewis et al., 2019). In the MeHg+Se co-exposed group, only the expressions of Chrm4 were found to be up-regulated, which may be related to learning and memory impairment. Se may play an important protective role in the long-term learning and memory impairments caused by MeHg exposure.

The protein encoded by the differential gene Gnas in the calcium signaling pathway is Gα, which is one of the constituent subunits of the G-protein. As an important signal transduction protein, its main function is to activate glands in the G-protein coupled receptor signal transduction pathway. Cyclase catalyzes the conversion of ATP to cAMP, and cell proliferation is inhibited when the cAMP content in the cell increases. Increased cAMP concentrations induce protein kinase A activation, which activates voltage-dependent calcium channels in the cell membrane, facilitating calcium uptake into the cellular and sarcoplasmic reticulum, and ultimately, leading to calcium overload and neuronal apoptosis. In the MeHg-exposed group, pathological changes such as neuron coagulation, shrinkage, deep staining of the cytoplasm, and mitochondrial swelling were observed, while the neuronal damages in the MeHg+Se co-exposed group was significantly reduced. These alterations in the ultrastructure of the cerebellum caused by MeHg exposure may be related to the significant changes in the calcium signaling pathway, since no related differential genes were found in the MeHg+Se co-exposed group.

Through screening of the DEGs with the high-throughput sequencing technology, the highest levels of statistical significance were identified for the “neuroactive ligand receptor interaction” and “calcium signaling” pathways altered by MeHg exposure. In the MeHg+Se co-exposed group, the numbers of DEGs were significantly reduced, but the DEGs were not directly related to nerve information transmission. In addition, down-regulated DEGs were mainly immune-related, and the functions and processes of these altered genes in the MeHg+Se co-exposed group cannot be fully explained in this study. The altered genes are rarely neurotransmitter-related, which suggests that Se has a protective effect against the neurotoxic effects of MeHg. Our study were consistent with previous findings, which found that short-term exposure to MeHg in rats mainly affected information transmission in CNS as well as the transmission and expression of genetic information (Jayashankar et al., 2011) The DEGs in the MeHg-exposed group were primarily involved in cell proliferation and the stress responses, while the DEGs in the MeHg and SeMet co-exposed groups were primarily involved in cell adhesion and synaptic and immune response signaling The findings in this study indicated that combined exposure to MeHg and Se inhibits the effect of MeHg on neuronal information transmission, which underlies the protective effect of Se on rat offspring.

4. Conclusions

MeHg exposure affects the body weight of rat offspring, reduces their survival rate, and leads to pathological changes in the morphology and ultrastructure of cerebellar neurons. The main signaling pathways related to cerebellar damage caused by MeHg exposure are the neuroactive ligand-receptor interaction and calcium signaling pathway, which are closely related to learning and memory impairment and cell apoptosis. Co-exposure to MeHg and Se alters the DEGs in related signaling pathways caused by MeHg damage. These findings demonstrated that Se alleviates neuronal damage caused by MeHg exposure by altering gene expression profiles associated with neural signaling and calcium signaling pathways. Overall, Se supplementation provides significant protection against MeHg-induced learning and memory impairment, especially in the developing cerebellum.

CRediT authorship contribution statement

Rui Tu: Data curation, Formal analysis, Investigation, Writing – original draft, Writing – review & editing. **Chanchan Zhang**: Data curation, Investigation. **Ling Feng**: Formal analysis, Investigation. **Huiqun Wang**: Methodology, Supervision. **Wenjuan Wang**: Methodology, Supervision, Writing – original draft, Writing – review & editing. **Ping Li**: Conceptualization, Funding acquisition, Investigation, Supervision, Writing – review & editing.

Declaration of Competing Interest

The authors declare that they have no known competing financial interests or personal relationships that could have appeared to influence the work reported in this paper.

Acknowledgments

This study was funded by the National Natural Science Foundation of China (U1812403, 81703191, and 41622208), the CAS Interdisciplinary Innovation Team (JCTD-2020-20), the Youth Innovation Promotion Association, Chinese Academy of Sciences (2017442), and the Chinese Academy of Sciences “Light of West China” Program.

Appendix A. Supporting information

Supplementary data associated with this article can be found in the online version at doi:10.1016/j.ecoenv.2021.112584.

References

Beyrouty, P., Chan, H.M., 2006. Co-consumption of selenium and vitamin E altered the reproductive and developmental toxicity of methylmercury in rats. Neurotoxicol. Teratol. 28, 49–58.
Buhot, M.C., Martin, S., Segu, L., 2000. Role of serotonin in memory impairment. Ann. Med. 32, 210–221.
Dantzig, P.I., 2003. A new cutaneous sign of mercury poisoning. Ann. Intern. Med. 139, 78–80.
Dreiem, A., Seegal, R.F., 2007. Methylmercury-induced changes in mitochondrial function in striatal synaptosomes are calcium-dependent and ROS-independent. Neurotoxicology 28, 720–726.
Driscoll, C.T., Mason, R.P., Chan, H.M., Jacob, D.J., Pirrone, N., 2013. Mercury as a global pollutant: sources, pathways, and effects. Environ. Sci. Technol. 47, 4967–4983.
Franco, J.L., Braga, H.C., Stringari, J., Missau, F.C., Posser, T., Mendes, B.G., Leal, R.B., Santos, A.R., Dafre, A.L., Pizzolatti, M.G., Farina, M., 2007. Mercurial-induced hydrogen peroxide generation in mouse brain mitochondria: protective effects of quercetin. Chem. Res Toxicol. 20, 1919–1926.
Genchi, G., Sinicropi, M., Carocci, A., Lauria, G., Catalano, A., 2017. Mercury exposure and heart diseases. Int. J. Environ. Res. Public Health 14, 74.
Grotto, D., Barcelos, G.R., Valentini, J., Antunes, L.M., Angeli, J.P., Garcia, S.C., Barbosa F, Jr, 2009. Low levels of methylmercury induce DNA damage in rats: protective effects of selenium. Arch. Toxicol. 83, 249–254.
Jayashankar, S., Glover, C.N., Folven, K.I., Brattelid, T., Hogstrand, C., Lundebye, A.K., 2011. Cerebral gene expression in response to single or combined gestational

exposure to methylmercury and selenium through the maternal diet. Cell Biol. Toxicol. 27, 181–197.
Johansson, C., Castoldi, A.F., Onishchenko, N., Manzo, L., Vahter, M., Ceccatelli, S., 2007. Neurobehavioural and molecular changes induced by methylmercury exposure during development. Neurotox. Res. 11, 241–260.
Joseph, L., Thomsen, M., 2017. Effects of muscarinic receptor antagonists on cocaine discrimination in wild-type mice and in muscarinic receptor M1, M2, and M4 receptor knockout mice. Behav. Brain Res. 329, 75–83.
Karita, K., Sakamoto, M., Yoshida, M., Tatsuta, N., Nakai, K., Iwai-Shimada, M., Iwata, T., Maeda, E., Yaginuma-Sakurai, K., Satoh, H., Murata, K., 2016. Recent epidemiological studies on methylmercury, mercury and selenium. Nihon Eiseigaku Zasshi 71, 236–251.
Kaur, P., Schulz, K., Aschner, M., Syversen, T., 2007. Role of docosahexaenoic acid in modulating methylmercury-induced neurotoxicity. Toxicol. Sci. 100, 423–432.
Koeman, J.H., Peeters, W.H., Koudstaal-Hol, C.H., Tjioe, P.S., de Goeij, J.J., 1973. Mercury-selenium correlations in marine mammals. Nature 245, 385–386.
Kruse, A.C., Hu, J., Pan, A.C., Arlow, D.H., Rosenbaum, D.M., Rosemond, E., Green, H.F., Liu, T., Chae, P.S., Dror, R.O., Shaw, D.E., Weis, W.I., Wess, J., Kobilka, B.K., 2012. Structure and dynamics of the M3 muscarinic acetylcholine receptor. Nature 482, 552–556.
Lee, J.H., Chiang, S.Y., Nam, D., Chung, W.S., Lee, J., Na, Y.S., Sethi, G., Ahn, K.S., 2014. Capillarisin inhibits constitutive and inducible STAT3 activation through induction of SHP-1 and SHP-2 tyrosine phosphatases. Cancer Lett. 345, 140–148.
Lewis, C.R., Henderson-Smith, A., Breitenstein, R.S., Sowards, H.A., Piras, I.S., Huentelman, M.J., Doane, L.D., Lemery-Chalfant, K., 2019. Dopaminergic gene methylation is associated with cognitive performance in a childhood monozygotic twin study. Epigenetics 14, 310–323.
Li, Y.F., Dong, Z.Q, Chen, C.Y, Li, B., Gao, Y.X, Qu, L.Y, Wang, T.C, Fu, X., Zhao, Y.L, Chai, Z.F, 2012. Organic selenium supplementation increases mercury excretion and decreases oxidative damage in long-term mercury-exposed residents from Wanshan, China. Environ. Sci. Technol. 46, 11313–11318.
Liu, Y.P., Wu, X., Meng, J.H., Ding, M., Xu, F.L., Zhang, J.J., Yao, J., Wang, B.J., 2019. Transcription factor CEBPB Inhibits the expression of the human HTR1A by binding to 5′ regulatory region in vitro. Genes 10.
Mergler, D., Anderson, H.A., Chan, L.H., Mahaffey, K.R., Murray, M., Sakamoto, M., Stern, A.H., Panel on Health Risks and Toxicological Effects of, M., 2007. Methylmercury exposure and health effects in humans: a worldwide concern. Ambio 36, 3–11.
Michalski, R., Pecyna-Utylska, P., Kernert, J., 2021. Determination of ammonium and biogenic amines by ion chromatography. A review. J. Chromatogr. A. 1651, 462319.
Osuna, C.E., Grandjean, P., Weihe, P., El-Fawal, H.A., 2014. Autoantibodies associated with prenatal and childhood exposure to environmental chemicals in Faroese children. Toxicol. Sci. 142, 158–166.
Pamphlett, R., Kum Jew, S., Cherepanoff, S., 2019. Mercury in the retina and optic nerve following prenatal exposure to mercury vapor. PLoS One 14, 0220859.
Ralston, N.V., Raymond, L.J., 2010. Dietary selenium's protective effects against methylmercury toxicity. Toxicology 278, 112–123.
Robinson, M.D., Oshlack, A., 2010. A scaling normalization method for differential expression analysis of RNA-seq data. Genome Biol. 11, 25.
Sakamoto, M., Chan, H.M., Domingo, J.L., Koriyama, C., Murata, K., 2018. Placental transfer and levels of mercury, selenium, vitamin E, and docosahexaenoic acid in maternal and umbilical cord blood. Environ. Int. 111, 309–315.
Sakamoto, M., Yasutake, A., Kakita, A., Ryufuku, M., Chan, H.M., Yamamoto, M., Oumi, S., Kobayashi, S., Watanabe, C., 2013. Selenomethionine protects against neuronal degeneration by methylmercury in the developing rat cerebrum. Environ. Sci. Technol. 47, 2862–2868.
Schrauzer, G.N., 2000. Selenomethionine: a review of its nutritional significance, metabolism and toxicity. J. Nutr. 130, 1653–1656.
Sun, Y.F, Zhou, Q., Zheng, J., 2019. Nephrotoxic metals of cadmium, lead, mercury and arsenic and the odds of kidney stones in adults: An exposure-response analysis of NHANES 2007-2016. Environ. Int. 132, 105115.
Tain, Y.L., Lin, Y.J., Chan, J., Lee, C.T., Hsu, C.N., 2017. Maternal melatonin or agomelatine therapy prevents programmed hypertension in male offspring of mother exposed to continuous light. Biol. Reprod. 97, 636–643.
Tsunoda, M., Johnson, V.J., Sharma, R.P., 2000. Increase in dopamine metabolites in murine striatum after oral exposure to inorganic but not organic form of selenium. Arch. Environ. Contam. Toxicol. 39, 32–37.
Wells, E.M., Herbstman, J.B., Lin, Y.H., Jarrett, J., Verdon, C.P., Ward, C., Caldwell, K.L., Hibbeln, J.R., Witter, F.R., Halden, R.U., Goldman, L.R., 2016. Cord blood methylmercury and fetal growth outcomes in baltimore newborns: potential confounding and effect modification by omega-3 fatty acids, selenium, and sex. Environ. Health Perspect. 124, 373–379.
Yeh, K.C., Hung, C.F., Lin, Y.F., Chang, D.C., Pai, M.S., Wang, S.J., 2020. Neferine, a bisbenzylisoquinoline alkaloid of Nelumbo nucifera, inhibits glutamate release in rat cerebrocortical nerve terminals through 5-HT1A receptors. Eur. J. Pharmacol. 889, 173589.
Zhu, J., et al., 2008. Distribution and transport of selenium in Yutangba, China: impact of human activities. Sci Total Environ. 252–261.